Miodrag D. Milenković-Babić
Head of section for aerodynamic and control
Military Technical Institute (VTI) Belgrade

Vanja D. Stefanović-Gobeljić
Research Engineer
Military Technical Institute (VTI) Belgrade

Branislav G. Ostojić
Research Engineer
Military Technical Institute (VTI) Belgrade

Biljana Z. Dovatov
Head of section for aeroelastisity and load
Military Technical Institute (VTI) Belgrade

Branislava B. Ostić
Research Engineer
Military Technical Institute (VTI) Belgrade

Maja B. Gligorijević
Research Engineer
Military Technical Institute (VTI) Belgrade

The Rescue System Implemetation in the Medium Range UAV

The modern approach to aircraft designs increasingly involves the application of rescue systems in crewed aircraft such as gliders, ultralight and trainer aircraft. Similarly, various classes of UAVs (unmanned aerial vehicles) are increasingly being equipped with parachutes or parachute-airbag landing systems. Whether the objective is to facilitate routine landings or to safeguard the UAV system and its components during recovery, integrating a parachute system serves as a vital solution. This paper presents an implementation analysis of the different rescue systems in medium-range UAV, addressing various limitations such as minimal mass increase, limited space within the UAV to house the system, changes to the center of gravity, stability and control considerations, and overall UAV performance. The paper also studies the capability of lateral-directional flight control surfaces compensation for the asymmetric load caused by the integrated one version of the rescue system under the wing, and performance of the required maneuvers in accordance with flight regulations.

Keywords: *UAV, rescue system implementation, composite structure modification, aerodynamic, flight control.*

1. INTRODUCTION

Today's designers of aircraft and unmanned aerial ve–hicles (UAVs) are placing greater emphasis on safety during the early stages of preliminary design. This inc–ludes considerations such as minimizing the take-off weight to ensure compliance with the safety levels required by airworthiness design standards [1]. One of the simplest ways to ensure safety with potential system mualfunctions is by integrating a parachute rescue sys–tem [2]. It has become common practice to include recovery systems in the all new-designed gliders, ultra–lights, trainer aircraft and UAVs. These systems can also be retrofitted later.

There is extensive research on the feasibility of integrating recovery systems into commercial aircrafts [3] and UAVs [4]. Parachute systems are often included in UAVs for routine landings at the end of missions [5], which depends on UAV category. In some cases, the UAV may become uncontrollable, making it impossible to land or position the UAV for rescue system activation. Therefore, parachute systems must be reli–able and well-integrated into the aircraft or UAV to ensure they can protect lives, minimize damage to the expensive, cutting-edge technology onboard and da–mage to other people's property. Implementing a rescue system in UAVs can significantly reduce the likelihood of fatal accidents, such as the one described in [6].

The presented paper focuses on integrating the rescue system in the medium-range UAV [7]. It is a multi-functional intelligence and reconnaissance UAV system with an operational radius of more than 200 km, shown in Figure 1, whose technical characteristics are given in Table 1. The analysis in [4] was partly repeated in the next chapter and extended to include stability and control considerations and overall UAV performance change.

Figure 1. Medium range UAV

Table 1. UAVs technical characteristics

UAV	
Power	38 KW (52 BHP) two-cylinder, two-stroke boxer
Propeller	Wooden, two blades, pusher
Referent wing span	6.34 m
Length	5.580 m
Max. payload weight	54 kg
Max. takeoff weight	265 kg
Max. speed	160 - 180 km/h+
Operational altitude	2000 -3000 m

2. ANALYSIS OF THE RESCUE SYSTEM IMPLEMENTATION

The medium-range UAV features a fully composite structure with a rear-mounted engine, simplifying main–tenance and allowing for convenient placement of the

Received: June 2025, Accepted: July 2025
Correspondence to: Dr Miodrag Milenković-Babić
Military Technical Institute (VTI) Belgrade,
Ratka Resanovića 1, 11030, Belgrade, Serbia
E-mail: miodragmbm@yahoo.co.uk
doi: 10.5937/fme2503482M

payload in the front section of the fuselage. This design approach significantly reduces the influence of engine and propeller vibration on the payload. It provides better image quality transmitted to the ground control station and substantially increases the capability to detect, recognize, and identify the potential target. The wing's centre section is an integral part of the fuselage and was initially intended to house fuel tanks during the project's early stages. At that time, the parachute rescue system was planned to be located in the fuselage centre, behind the fuel tanks. However, a change in the design concept introduced a second fuel tank within the fuselage, leaving the space originally allocated for integral tanks unused and side-lining the parachute system. The initial plan to incorporate a rescue system was ultimately replaced by the need for additional fuel to extend endurance for two distinct mission profiles. The expected endurance for the reconnaissance mission was 10 hours, while for the armed mission was 6 hours.

In response to the new requirement for a rescue system, the analysis of two possible placement for parachute integration has been done:

1. **First approach**: The goal was to develop a solution using our own resources, in collaboration with subcontractors from domestic (Serbian) country.
2. **Second approach**: The aim was to identify a certified ballistic parachute system of foreign origin that is already in widespread use in various UAVs and ultralight aircraft.

Both approaches required a thorough investigation of the market and parachute manufacturers offering certified systems already in use, summarizes the data for the companies and products reviewed and analyzed. Table 2 presents the options that satisfy the specified requirements.

Table 2. Possible rescue system solutions

	Galaxy GRS GRS 4 270 60 m^2	**Galaxy GRS GRS 4 270 60 m^2**	**PR 03-1 Kluz**
Max. UAV mass [kg]	270	270	
Type of system	Ballistic	Ballistic	
Type of package	Soft	Out unit	Soft
Mass of the system [kg]	8.8	9.6	6
Dimension [mm]	195x245x305	Ø185x500	420x240x160
Max. dynamic impact [kN]	14.5	14.5	
Average UAV vertical speed [m/s]	6.6	6.6	
Parachute diameter [m]	7.2	7.2	
Parachute surface area [m^2]	60	60	45.5
Max. UAV airspeed [km/h]	230	230	
System volume [l]	14.6	13.4	16.2
System life cycle [repacking]	6 years	6 years	

2.1 First approach

Given that the maximum descent speed for a safe UAV landing must be less than 7 m/s and the UAV's maximal mass is 265 kg, a parachute with a minimum canopy area of 60 m² was required. However, the UAV lacked sufficient internal space to house a parachute of this size. The initial solution involved utilizing the only available space within the UAV: the center section of the wing, which offered two compartments with a combined volume of 30 liters (Figure 2).

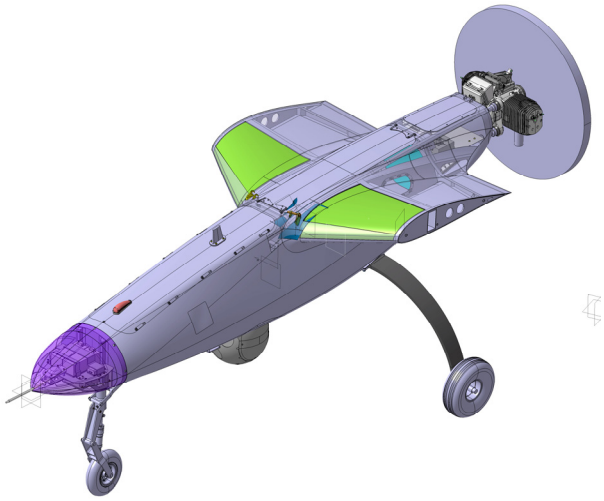

Figure 2. Free space for parachutes (green)

The decision was made to start the analysis with two smaller parachutes that could be obtained quickly. The available space in the center section of the wing was sufficient to accommodate two reserve parachutes, PR03-1, with a canopy area of 45.5 m². These parachutes were readily available for installation and testing. The system also includes two pilot parachutes with springs and two main parachutes, which will be connected together.

The just mentioned approach required the modification of the wing center section in order to accommodate a cover on the upper skin, and enable the easy deployment of the parachutes. Any additional modification to the wing would require a design optimization strategy and structural analysis [8]. A wind tunnel test could be conducted as a method for verifying the system's functionality. This test would simulate the deployment of the cover and the launching of the parachutes under flow conditions similar to those experienced during an actual in-flight rescue mission (Figure 3).

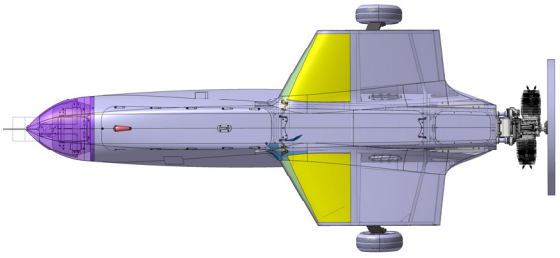

Figure 3. Cover on the upper skin (yellow)

The pilot parachutes will deploy at a sufficient height to clear the UAV's tail and empennage, carrying

the main parachutes with them. No additional numerical or flight tests will be necessary to evaluate aerodynamic changes, as all components of the system will remain enclosed within the fuselage. The parachute system will add 10 kg to the UAV's total weight. Since the parachutes will be positioned close to the center of gravity, the resulting shift in the center of gravity will be negligible. The additional weight of the implemented rescue system will require the reduction of the fuel capacity that can be available for different UAV missions.

2.2 Second approach

The second approach involved exploring the international market to identify the most suitable rescue system for this type of UAV. Various systems were evaluated, and contact was established with several companies. The companies that expressed interest are listed in Table 2. Prominent industry leaders, including BRS Aerospace, Junkers Magnum Rescue System, and Galaxy Rescue System, were among those contacted. For the medium-range UAV, only the Galaxy Rescue System (GRS) met the requirements, while the other two companies either discontinued production for this UAV category or did not offer suitable products. As the leading company in this market segment, GRS provided two parachute system options: the soft pack system and the OUT unit.

Several limitations were encountered, as each system includes a rocket as part of the parachute deployment mechanism. The best solution was to install the rocket at the top of the fuselage; however, the presence of front and rear fuel tanks made it impossible. Since pylons are already installed under the reinforced wings, and installation provisions for weapons are in place, only minor modifications would be needed to mount the OUT unit under the wing (Figure 4).

Figure 4. OUT unit attached to the wing pylon

The second option involved designing an integral container for the soft pack, mounting the rocket on it, and covering the system with an aerodynamically shaped cover. This would allow the system to be securely attached to the wing pylon (Figure 5). The integral container would be a weather-resistant pack, similar to the OUT unit. The final decision will depend on the availability of these systems, ease of use, and the drag force they produce, as the mass of both systems is approximately the same.

Similar to the armed UAV, when the external parachute unit is incorporated into the mission, fuel reduction must be calculated to ensure that the maximum UAV mass remains within 265 kg. An advantage of this approach is that the integration of any rescue system will not affect the center of gravity. The system features electronic activation, and the unit will be installed inside the UAV, specifically in the left wing.

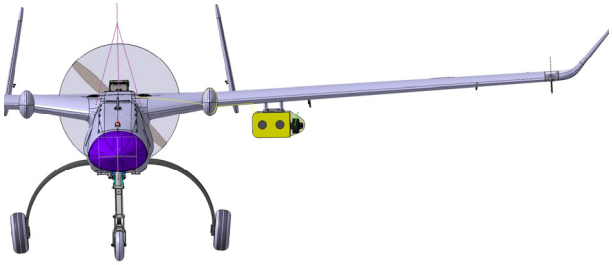

Figure 5. Integral container with soft pack and rocked attached to the wing pylon

In both variants, the attachment points will be positioned at three locations on the fuselage: two in front of the center of gravity and one behind it. Figure 6 illustrates the placement of the attachment points, with the center of gravity indicated by a yellow sphere. Before testing the rocket and parachute deployment, some numerical calculations need to be conducted.

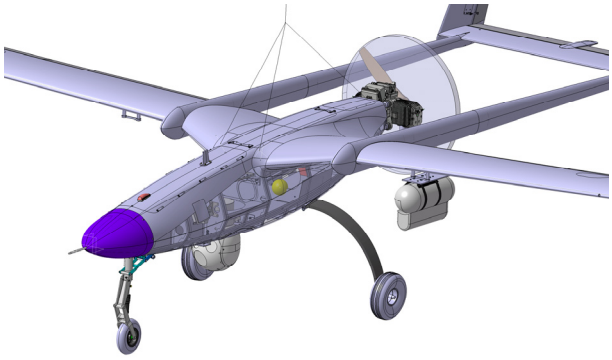

Figure 6. Hanging points and centre of the gravity

Since the masses of the rescue systems are smaller than those of the weapons, which have already been accounted for in the static strength calculations of the wing and pylon, a static strength verification will not be required. The calculation of the aerodynamic drag resulting from the attachment of these rescue systems, as described in the second approach, is presented in the next chapter.

3. AERODYNAMIC DRAG ESTIMATION

To determine which rescue system has the minimal influence on UAV performance, an aerodynamic analysis was conducted. Computational fluid dynamics (CFD) simulations of the drag force for the rescue systems were performed using the commercial ANSYS Fluent software, employing finite volume methods. Numerical simulation methods have been widely and successfully applied to compressible turbulent flow problems [9, 10]. Several turbulence models are available, with low-order models generally being less accurate than high-order ones. Since it was necessary to estimate the drag force with sufficient accuracy, the k–ω SST turbulence model was used. Calculated reference surface area was 4.24 m².

The working fluid was defined as ideal gas (air). The computations were performed until the convergence criteria were met. The reference data used for the simu–lations are presented in Table 3.

Table 3. Data for simulation

Data for simulation	
Altitude	3000 m
Flight speed	42 m/s
Pressure	70109 Pa
Density	0.909 kg/m^3
Kinematic viscosity	1.861 x 10^{-5} m^2/s

4. FLIGHT ENDURANCE ESTIMATIN

Implementation of the rescue system will significantly change the UAV's mass and inertia properties. The UAV's capabilities will be reduced, and the most signi–ficant characteristic that needs to be evaluated is flight endurance. The effects that need to be considered are:

- The maximal UAV's weight that cannot be exce–eded. This limit will require the reduction of the usable weight of fuel that can be put in UAVs.
- Stability and control characteristics in lateral-dire–ctional motion.
- Change in UAV's drag and trim drag charac–teristics.

The implemented solution for the rescue system is equivalent to the external weapons that are integrated into many UAVs and aircraft. It will produce the addi–tional parasitic drag that is estimated using the well-known components build-up method. This method is excellently summarized in Dr. Raymer's book [11], and for streamlined body software like Open-VSP [12] can be used. It is NASA's conceptual design software that can be used for estimating the parasitic drag. It can esti–mate the body drag force coefficient at a variety of atmospheric conditions, skin friction factors, and form factor equations.

As it is well-known and mentioned in Dr. Raymer's book [11], skin friction drag is significantly affected by the laminar flow over the body surfaces. It can double if the flow becomes turbulent instead of laminar. In many aeronautical cases, the transition from laminar to turbu–lent flow occurred near the front of the UAVs as a consequence of the integrated payload. The payload usually is not the streamlined body and it produces the transition in boundary layer flow and airflow separation that increases drag force significantly.

The equation for estimating the flight endurance that represents one of the most important flight charac–teristics can be found in many books and one excellent example is [13] that will be used in the presented example. In [13] it is shown that any flight could be divided into a few segments. Each segment is clearly distinguished from others by its nature. The differential equation that can be used for every flight segment is:

$$dt = \frac{-1}{c_t T} dW \tag{1}$$

The previous equation could be solved through the numerical integration with the limits that are the initial and final weights during the analyzed segment. It is the well-known "Breguet" endurance equation in which the t represents time, c_t represents thrust-specific fuel consumption [1/sec], T represents thrust [N], and W represents the UAV's weight [N]. The specific fuel consumption is provided by the engine manufactured company [14] by the experimental measurement.

In order to solve the "Breguet" endurance equation additional assumptions should be made. In the presented paper, a constant airspeed and constant attitude cruise is assumed, and it leads to the range equations in the simple form:

$$R_{cScA} = \frac{V}{c_t}\frac{C_L}{C_D}\ln\left(\frac{W_{initial}}{W_{final}}\right) \tag{2}$$

where the C_L is UAV's lift force coefficient, C_D is the UAV's drag force coefficient, and $W_{initial}$ and W_{final} rep–resent the initial and final weights of the UAV, respec–tively.

5. STABILITY AND CONTROL

The integration of the rescue system will affect the available control surface deflection for different mane–uvers, and it is necessary to estimate its effects during critical flight phases. As is well known, the required control deflection is inversely proportional to the UAV's airspeed squared. Therefore, the minimum flight speed, which is typically the landing airspeed, will be analyzed in this paper. The lateral-directional dynamics are well summarized in textbooks by Perkins [15], DATCOM [16], Smetana [17], and in various papers [18-21]. The estimation of flight control deflection (for the ailerons and rudder) during straight, level flight can be calculated using the following equation:

$$\delta_a = \frac{m_{payload}\cdot g\cdot b_{payload}}{C_{l_{\delta_a}}\cdot q\cdot S\cdot b},$$
$$\delta_r = \frac{C_{D_{payload}}\cdot S_{payload}\cdot b_{payload}}{C_{n_{\delta_r}}\cdot S\cdot b} \tag{3}$$

When calculating the additional drag of the rescue system (payload), the interference factor with the wing must be taken into account. This will increase the drag force coefficient by a value that can be found in Hoerner's book [22]. The airworthiness requirements for this class of UAV system are outlined in [23]. This airworthiness code primarily applies to fixed-wing UAV systems with a maximum take-off weight of more than 150 kg and less than 20,000 kg.

This regulation specifies that, in automatic control mode, the UAV must demonstrate acceptable contro–llability, maneuverability, and stability characteristics throughout the flight envelope. However, the regulation [23] does not include any requirements for the rate of roll, so additional regulations must be referenced to estimate UAV characteristics in this flight phase. For this purpose, SC-23 [24] can be used as a guide for UAV roll performance. The regulation [24] requires that, during the approach phase, the aircraft roll from a

steady 30° banked turn through an angle of 60° to reverse the direction of the turn within 4 seconds from the initiation of the roll, for aircraft with a maximum weight of less than 2722 kg. The roll rate can be estimated using the roll mode approximation [25, 26]:

$$\ddot{\varphi} \cdot I_x = QSb \cdot \left(\frac{b}{2 \cdot V} \cdot C_{lp} \cdot p + C_{l\delta_a} \cdot \delta_a \right) \tag{4}$$

If stationary roll has been assumed ($\ddot{\varphi} = 0$, p = const), then the steady state roll rate is defined by equation [19]:

$$p = \dot{\varphi} = \frac{4QSbC_{l\delta_a}\delta_a}{\rho V S b^2 C_{lp}} = \frac{2V}{b}\frac{C_{l\delta}}{C_{lp}}\delta_a \tag{5}$$

Paragraph 233 (Directional Stability and Control) requires that a 90° crosswind component of at least $0.2V_{S0}$ is considered safe for taxiing (except for UAVs not designed for taxiing), takeoff, and landing. This can be estimated using the following equation:

$$V_w = V_{S0} \cdot tg\beta = V_{S0} \cdot tg\left(-\frac{C_{n\delta r}}{C_{n\beta}} \cdot \delta_r \right) \tag{6}$$

Despite the complexity of lateral-directional dynamics [20], the aerodynamic lateral control power coefficient, aerodynamic lateral roll damping coefficient, weathercock effect, and yawing moment coefficient associated with rudder deflection can be estimated using data from textbooks [15-17,27] or through computational fluid dynamics (CFD) [10,28]. The roll damping coefficient is typically considered constant with respect to roll rate [21], and it can be accurately evaluated using the methods described in [15-17,27], rather than numerically through CFD methods. Therefore, in the presented analysis, it will not be evaluated using CFD.

For the evaluation of aileron and rudder surface deflections, data from CFD simulations [28] have been used to obtain more accurate results. Since the maximum aileron deflection does not exceed 17°, the recommendation in [21] regarding the nonlinearity factor is unlikely to have a significant effect on the UAV's rolling capabilities.

6. RESULTS AND DISCUSION

To determine the optimal position for integrating the rescue system, various possibilities were analyzed. The rear and front positions were deemed inadequate due to their adverse effects on the UAV's center of gravity and the limited space available for the rescue system. The central part of the wing section offers adequate volume for integration; however, the main drawback is that it is split between the left- and right-wing sections, requiring two small, independent parachutes and additional wing modifications. This option will be subject of further researches including analysis of fuselage modification and testing in the wind tunnel.

The wing attachment point was considered as another potential solution. This position would not significantly affect the UAV's center of gravity, as the attachment points are located near the center of gravity. For these reasons, the attachment point under the left wing was chosen as the optimal solution and was analyzed in detail in this paper.

The additional fuel weight reduction due to the rescue system integration was estimated to be 11 kg, which is equivalent to the weight of the parachute rescue system. The results indicate a noticeable decrease in the usable fuel mass. The parachute-based rescue system adds 4.2% to the UAV's total weight, which means that integrating the rescue system requires a corresponding reduction in the available fuel by the same percentage.

Using the Component Build-Up Method, the additional drag caused by the integrated rescue system was estimated using data from Table 12.6 in [11]. It was assumed that the integrated rescue system would have a similar drag force coefficient to a bullet-shaped body with a blunt rear end. The parasite drag force coefficient for the integrated rescue system was estimated to be C_D=0.3, based on the reference frontal area. Computational fluid dynamics (CFD) simulations estimated the drag force values as 13.994 N for the integral container and 16.917 N for the OUT unit. The reference surface area was defined as 4.24 m², and it was assumed that the UAV was flying at an altitude of 3000 m with an airspeed of 42 m/s. The dynamic pressure distribution on the surface of the OUT unit was found to be of lower intensity compared to the pressure on the surface of the integral container (Figure 7).

The estimated drag force coefficient for the integral container, based on the reference rescue system's frontal area, is C_D=0.29091. This result shows excellent agreement with the value reported in reference [11] (C_D=0.3), with an error of up to 3%. This small error is unlikely to affect the estimated performance results. The approach presented for estimating UAV flight performance has been successfully applied to the medium-range UAV's flight performance estimation and verification, as detailed in [10, 28-30].

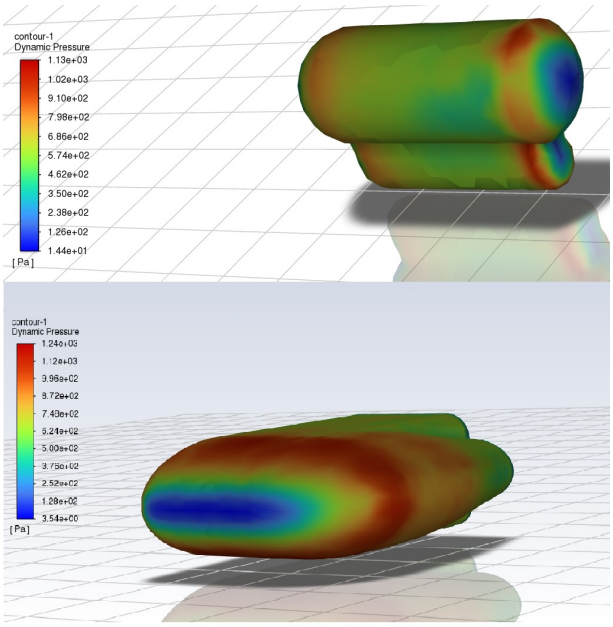

Figure 7. Dynamic pressure distribution of OUT unit (upper) and integral container (lower)

The results of the UAV flight endurance, both with and without the rescue system, are provided in Table 4 as a function of UAV airspeed.

Table 4. Estimated endurance results without and with rescue system

V [km/h]	t_{cScA} [h]	t_{cScA} [h]
135	12.92	9.89
150	12.03	9.14

Since the additional drag force of the OUT unit has an insignificant effect on the endurance estimation, it will not be analyzed further in this paper.

The reduction in usable fuel from 70 kg to 59 kg results in an endurance decrease of 17.8%. The additional drag from the integrated parachute rescue system further reduces endurance by 5.6–6.2%. If the UAV could carry the same amount of fuel while having the integrated rescue system attached under the left-wing pylon, the flight endurance would only be reduced by 6%.

The estimated stability and control derivatives, calculated using different methods for the medium-range UAV, are shown in Table 5. The CFD derivatives have been estimated using the following equations:

$$C_{l\delta_a} = \frac{C_{l_{(\alpha=0°,\delta_a=5°)}} - C_{l_{(\alpha=0°,\delta_a=0°)}}}{5} \cdot 57.3$$
$$C_{n\delta_r} = \frac{C_{n_{(\alpha=0°,\delta_r=5°)}} - C_{n_{(\alpha=0°,\delta_r=0°)}}}{5} \cdot 57.3 \qquad (7)$$
$$C_{n_\beta} = \frac{C_{n_{(\beta=5°,\alpha=0°)}} - C_{n_{(\beta=0°,\alpha=0°)}}}{5} \cdot 57.3$$

The accuracy of the presented method has been verified by comparing the estimated results for X-tail UAV control derivative with the wind tunnel test result on the full-scale UAV model [31].

Table 5. Estimated results of the stability and control derivatives with the diffrent methods

	Smetana [17]	CFD [28]	DATCOM [16]
$C_{l\delta_a}\,(1/rad)$	0.1719	0.198	0.1662
$C_{n\delta_r}\,(1/rad)$	0.1068	0.13	0.1031
$C_{lp}\,(1/rad)$	-0.452	-0.452	0.4186
$C_{n_\beta}\,(1/rad)$	0.1862	0.1552	0.1434

The rudder deflection required to compensate for the yawing moment of the rescue system is estimated to be 0.528°. Since the maximum rudder deflection is 30°, this will not affect the UAV's ability to compensate for the cross-component of wind. According to regulation [24], the required value for the crosswind component is $0.2V_{S0}$=5 m/s. The estimated result for the worst-case scenario indicates that the maximum crosswind component that can be compensated is not less than 6.4 m/s.

The servo actuators [32] used in the UAV provide a speed of over 200°/s in continuous mode. With a maximum deflection of 45° in one direction, the time to achieve this deflection is less than 0.225 seconds. The aileron deflection required to compensate for the rolling moment of the rescue system (gravity component) is estimated at 3.34°. The steady-state roll rate is estimated to be 21.33°/s, which is a reduction from 26.55°/s without the rescue system integrated under the left wing. Despite this reduction in the UAV's rolling capability, the analysis shows that it can still meet the CS-23 regulation. The UAV is able to roll from a steady 30° banked turn through an angle of 60°, reversing the direction of the turn within 4 seconds. To verify the actual UAV capabilities [33], flight tests should be conducted [34].

7. CONCLUSION

The integration of parachute rescue systems, which have become an inevitable part of many flying object, was analyzed in this paper. Based on data obtained from numerical simulations, it was found that the integral container produces a lower overall drag force, but not by a significant amount.

The estimated masses of the two systems are similar; however, the integration process and the time required for the systems to become functional suggest that the OUT unit has an advantage over the integral container with an aerodynamically shaped cover. In the case of the integral container, it is necessary to produce the container and cover, purchase the parachute and rocket, and perform system verification. On the other hand, the OUT unit offers a faster and more straightforward solution, as it comes pre-packaged with the cover and requires minimal testing for approval. Nevertheless, further research and testing will clarify which option is more efficient in practice.

The lateral directional dynamic analysis showed that the integration of the rescue system will affect the UAV's rolling capabilities, but it will have an insignificant impact on its ability to compensate for crosswind components.

The method presented in this paper provides accurate results and is easy to implement for evaluation of the lateral directional control authority of the UAV, particularly during terminal flight phases such as aborted landings. The safe flight envelope can be defined using these methods, based on a comparison between the available deflections of the flight control surfaces and the required deflections needed to satisfy regulatory requirements.

ACKNOWLEDGMENTS

This work was supported by the Ministry of Science, Technological Development and Innovation, Republic of Serbia (Contract No.451–03–137/2025–03/200325).

REFERENCES

[1] Casarosa, C., Galatolo, R., Mengali, G. and Quarta, A.: Impact of safety requirements on the weight of civil unmanned aerial vehicles, Aircraft Engineering and Aerospace Technology, Volume 76, Number 6 600–606, 2004.

[2] https://nova.rs/vesti/hronika/oglasilo-se-ministarstvo-odbrane-o-misterioznim-dronovima-kod-kraljeva/.

[3] Bolonkin, A.: Passenger life-saving in a badly damaged aircraft scenario, Aircraft Engineering and Aerospace Technology, 80/6, 613-119, 2008.

[4] Stefanović-Gobeljić, V., Milenković-Babić, M. and Zdravković, M.: Analysis of the rescue system implementation in the medium range UAV, 11th international scientific conference on defensive technologies OTEH 2024, Serbia, Tara, 80-85, October 2024.

[5] Antonić, V., Trifković, M., Molović, V. and Milenković-Babić, M.: Small fixed-wing UAV precision aerial drop capability development, Scientific Technical Review, 2024, Vol. 74, No. 2, pp. 65-70, 2024.

[6] https://edition.cnn.com/world/live-news/ahmedabad-india-plane-crash-06-12-25.

[7] Milenković-Babić, M., Ivković, D., Ostojić, B., Trifković, M., Antonić, V.: Take-off and landing performance of the tactical UAV, Scientific Technical Review, Vol.73, No.2, pp. 7-12, 2023. DOI: 10.5937/str2302004M

[8] Farah, S., Khalfallah, S., Boutemedjet, A., Rebhi, L.: A Design Optimization Strategy of an Aircraft Composite Wing-Box Based on a Multi-scale FEA, FME Transactions, Vol. 53, No 1, pp. 157-172, 2025.

[9] Gavrilović, N, Rašuo, B., George S Dulikravich, G., Parezanović, V.: Commercial Aircraft Performance Improvement Using Winglets. FME Transactions, 2015, 43 (1), pp.1-8.

[10] Milenković-Babić, M., Dovatov, B., Ostojić, B. et all.: Tactical UAV flight performance estimation and validation, Defence Science Journal, Vol. 75, No. 1, pp. 19-26, January 2025.

[11] Raymer, D.: Aircraft Design: A Conceptual Approach, Fifth edition, AIAA education series, 2012.

[12] https://openvsp.org/.

[13] Snorri, G.: General Aviation Aircraft Design: Applied Methods and Procedures. Elsevier Inc, 2014.

[14] Zanzottera Engines. 630HS Engine. Retrieved from https://www.zanzotteraengines.com/engines/630hs-engine/.

[15] Perkins, C.D., Hage, R.E.: Airplane performance stability and control, John Wiley& Sons, New York, 1949.

[16] USAF stability and control DATCOM, McDonnell Douglas Corporation, Douglas Aircraft Division, 1978.

[17] Smetana, F.: Computer assisted analysis of aircraft performance stability and control, McGraw-Hill, New York, 1984.

[18] Stojaković, P., Rašuo, B.: Single propeller airplane minimal flight speed based upon the lateral maneuver condition, Aerospace Science and Technology. 49 (2016), pp. 239–249.

[19] Stojaković, P., Rašuo, B.: Minimal safe speed of the asymmetrically loaded combat airplane, Aircraft Engineering and Aerospace Technology, 2016, Vol.88, No.1, pp. 42 – 52.

[20] Stojaković, P., Velimirović, K., Rašuo, B.: Power optimization of a single propeller airplane take-off run on the basis of lateral maneuver limitations, Aerospace Science and Technology, 72 (2018), pp. 553-563.

[21] Nicolasi, F., De Marco, A., Sabetta, V., Della Vecchia, P.: Roll performance assessment of a light aircraft: Flight simulations and flight tests, Aerospace Science and Technology, Vol. 76, pp. 471-483, 2018.

[22] Hoerner, S.: Fluid dynamic drag, theoretical, experimental and statistical information (Published by the author), 1965.

[23] STANAG 4671 – Unmanned aerial vehicles systems airworthiness requirements, 2009.

[24] EASA CS-23. Certification specifications for normal, utility, aerobatic and commuter category aeroplanes, 2014.

[25] Cook, M.: Flight Dynamics Principles, Third Edition, Elsevier Ltd., 2013.

[26] Blakeloock, J.: Automatic control of aircraft and missiles, Second edition, John Wiley & Sons, 1991.

[27] Napolitano, M.: Aircraft Dynamics: From Modeling to Simulation, Wiley, 2021.

[28] B3–600-P-06, Proračun aerodinamičkih karakteristika taktičke bespilotne letelice srednjeg doleta - PEGAZ, primenom CFD-a, VTI,

[29] Beograd, 2020. (in Serbian)

[30] Даљински пилотирани ваздухоплов ПЕГАЗ–перформансе. VTI report No. В3–602-П-06, 2020.

[31] Даљински пилотирани ваздухоплов ПЕГАЗ – извештај о земаљским и летним испитивањима. VTI report No. В3–602-И-06, 2022. (in Serbian)

[32] Milenković-Babić, M., Ostojić, B., Dovatov, B. et all.: Control derivative estimation of X-tail control surface design, Aerospace Science and Technology. 163 (2025). Available online 16 May 2025

[33] DA 26 Technical Specification, Volz Servos GmbH & Co., www.volz□servos.com.

[34] Marin, M., Mirosavljević, P.: Analysis of the performance and kinematics of the movement of UAV, FME Transaction, Vol. 51, No 4, pp. 627-636, 2023.

[35] Milenković-Babić, M., Ivković, D., Ostojić, B. et all.: Flying Wing Conceptual Design and Flight Testing, FME Transactions, Vol. 52 No 4, 2024.

ИМПЛЕМЕНТАЦИЈА СИСТЕМА ЗА СПАШАВАЊЕ ЛЕТЕЛИЦЕ У СЛУЧАЈУ ФАТАЛНОГ ОТКАЗА

М.Д. Миленковић-Бабић, В.Д. Стефановић-Гобељић, Б.Г. Остојић, Б.З. Доватов, Б.Б. Остић, М.Б. Глигоријевић

Савремени приступ пројектовања летелица све чешће укључује примену система за спашавање летелица као што су: једрилице, ултра лаке летелице и летелице за почетни ниво обуке пилота. На исти начин, различите категорије беспилотних летелица су опремљене са падобраном или падобраном и ваздушним јастуком. Ови систем се могу користити за уобичајно приземљење летелице (слетање) или као део система за спашавање летелице и скупе опреме интегрисане у њу у случају фаталних отказа у систему. У овом раду је приказана могућност интеграције неколико различитих система за спашавање летелице средњег домета у случају фаталног отказа. Анализирани су различита ограничења као што су: минимално повећање масе, ограничени простор за уградњу система за спашавање летелице, промена положаја тежишта летелице, утицај на стабилност и управљивост и перформансе модификоване летелице. У раду је такђе приказана анализа ауторитета команди попречно смерног мода управљања услед асиметричног оптерећења које је поседица интеграције система за спашавање летелице испод левог крила. Анализиране су могућности задовољења захтева маневра из прописа за цивилну авиоацију јер у пропису за беспилотне летелице (STANAG 4671 – Unmanned aerial vehicles systems airworthiness requirements, 2009) нема ових захтева.